Thermal anomaly near the Aigio fault, Gulf of Corinth, Greece, maybe due to convection below the fault

M. L. Doan, F. H. Cornet

GEOPHYSICAL RESEARCH LETTERS, VOL. 34, L06314, doi:10.1029/2006GL028931, 2007

Thermal anomaly near the Aigio fault, Gulf of Corinth, Greece, maybe due to convection below the fault

M. L. Doan[1] and F. H. Cornet[2]

Received 28 November 2006; revised 4 February 2007; accepted 27 February 2007; published 31 March 2007.

[1] A thermal profile has been measured in a 1000 m deep borehole intersecting the active Aigio fault, Corinth Rift, Greece. The heat flow is 53 mW/m^2, indicating that the rifting process has no effect in heat flow. The temperature near the fault is higher than expected from a pure conductive model. This discrepancy is not due to fluid flow above the fault as shown by the long term monitoring of downhole pressure. Neither can it be attributed to the fault slip since the Aigio fault is a minor normal fault of the rift, with no very recent earthquake. We propose that the anomaly is due to the convection within the karst that constitutes the footwall. Numerical simulations give a correct estimate for the recorded temperature increase. This is an extreme case of thermal disturbance induced near a fault by local fluid circulation. The occurrence of convection outside geothermal area is very rare. **Citation:** Doan, M. L., and F. H. Cornet (2007), Thermal anomaly near the Aigio fault, Gulf of Corinth, Greece, maybe due to convection below the fault, *Geophys. Res. Lett.*, *34*, L06314, doi:10.1029/2006GL028931.

1. Introduction

[2] The Corinth Rift is a 120°N trending gulf separating Peloponnese from mainland Greece. It is one of the most active continental rift with a spreading rate of 1.5 cm/yr [*Avallone et al.*, 2004]. This extension is accompanied by intensive faulting on its southern shore.

[3] In spite of this geodynamical interest, no successful heat flow measurement has been conducted so far in the Rift because of intense fluid circulation in the shallower sedimentary layers of the Gulf (G. Bienfait, personal communication, 2004). The 1000 m deep AIG10 borehole drilled to study the Aigio fault raised hope of a reliable measurement of the regional heat flow. However, the intensively karstified limestone that extends below the fault complicated this attempt and no complete log could be done.

[4] Yet the temperature data yields an interesting phenomenon in the hanging wall: a larger than anticipated temperature is observed in the borehole from 600 m (200 m above the fault) to the fault depth. Classical explanations like fluid circulation or fault activity do not account for such a discrepancy. Indirect observations suggest that the karstic aquifer below the fault is in thermal convection. Numerical simulations with convection in the karst below the fault explain the thermal profile.

2. Thermal Anomaly in the AIG10 Borehole

[5] The motivation of this work is to improve the understanding the thermal state around the Aigio fault. In this section, we first summarize the tectonic context. Then, we present the thermal data and exhibit the thermal anomaly near the fault. Hypotheses other than convection in the footwall aquifer are finally discussed.

2.1. Aigio Fault and the AIG10 Borehole

[6] The Aigio fault is one of the youngest on-shore faults of the Corinth Rift, with a vertical displacement of 150 m. It drew attention when it slipped as a response of the M_s = 6.2 1995 ''Aigio'' earthquake, located more than 10 km to the North [*Bernard et al.*, 1997; *Koukouvelas*, 1998].

[7] The Aigio fault is the site of the 1000 m deep AIG10 borehole, installed within the framework of the Corinth Rift Laboratory (CRL) [*Cornet et al.*, 2004]. The well intersects the Aigio fault between 760 and 770 m. The dip of the fault is thus of 60° and does not seem to change with depth. Coring and various logs have been performed to constrain the geological and geophysical environment of the fault. Pore pressure in the well has been continuously measured from September 2003 to early 2005.

[8] Figure 1 shows the formations intersected by the borehole. The borehole intersects syn-rift conglomerates from the surface to the depth of 388 m. From 389 m to 760 m, the Olonos-Pindos nappe is observed. It is a layering of clays, radiolarite and limestone. This sequence is complicated by thin stratifications at smaller scale as the Pindos nappe is intensely deformed and overthrusted by the Alpine compression [*Rettenmaier et al.*, 2004]. However, the most homogeneous layer of the Pindos nappe at the well extends over 50 m (between 696 and 760 m) above the fault. Below the fault extends the Tripolitza nappe. This layer of homogeneous limestone is heavily karstified. The thickness of the layer remains unknown as the bottom of the nappe is not reached by the borehole.

[9] The fault itself is characterized by a 1-meter thick clay gouge above 10 m of smeared radiolarites. Between the two layers, clear slickensides are visible. The fault separates two limestone layers that are more damaged within 10 m from the fault. The footwall is more damaged than the hanging wall. The difference in artesian pressure (0.4 MPa) between the two aquifers separated by the fault shows that the fault is an impermeable barrier between the aquifers, because of its layers of clayish gouge and radiolarite. This is also confirmed by the difference in mineralization between the two formations [*Frima et al.*, 2005].

[1]Earth and Planetary Sciences Department, University of California, Santa Cruz, California, USA.
[2]Department of Seismology, Institut de Physique du Globe de Paris, Paris, France.

0094-8276/07/2006GL028931

2.2. Thermal Profiles

[10] Four successful thermal profiles were performed within the AIG10 well.

[11] The first thermal information was provided through the UBI log Schlumberger performed only within two days after the completion of the borehole. A later OSG log was performed one week later. Its maximum temperature reaches 32.9°C. The bottom of the borehole was cooled by mud circulation during 17 h, so that the OSG log is done after a time span of 10 times the cooling duration. The temperature should not evolve more than 0.5°C.

[12] The borehole was then filled with mud and let undisturbed for 10 months. A second thermal log was then conducted with the equipment of Institut de Physique du Globe de Paris (IPGP). Temperature is recorded every 10 m with a thermal resistor at the end of a 3000 m-long cable of known resistance. The temperature resolution is better than 0.01°C. Unfortunately the lightness of the probe prevented its insertion below 200 m.

[13] With the help of IPGP engineers, GeoForschungs-Zentrum (GFZ) used the Distributed Temperature Sensing technology to perform a thermal profile on September 2003 (A. Förster et al., Petrophysical and temperature logging in the ICDP AIG10 borehole (Greece), Scientific Drilling Database, doi:10.1594/GFZ.SDDB.1091, 2006). Temperature-versus-depth data are obtained by Raman back-scattering and optical time-domain reflectometry within a fiber optics [*Förster et al.*, 1997]. Stacking data over time gives a precision of 0.3°C with one data point every meter. Comparison with the IPGP log shows that the temperature resolution reaches 0.1°C. The GFZ log extends down to the Aigio fault but stops at 750 m.

[14] All three logs are compiled in Figure 1. GFZ and IPGP logs document the upper part of the borehole. Their data coincide for the overlapping depth interval up to 200 m.

2.3. Thermal Paradox

[15] We have also measured in the laboratory the thermal conductivity of the matrix of the major facies encountered in the AIG10 borehole.

[16] The in-situ thermal conductivities are computed as a geometric average between the conductivity of the matrix and the conductivity of the water, equal to 0.6W/(K × m). The porosity of the in-situ formation is provided by a sonic log performed by Schlumberger. For the Pindos nappe extending from 496 m to 700 m, we also averaged the proportion of clay, limestone and radiolarite given by the cuttings log [*Rettenmaier and Unkel*, 2002]. Ampler information on the measurements is provided in the auxiliary material.[1]

[17] These values were integrated in the numerical model described in Figure 2. This model assumes pure conduction and ignores any heat advection by fluid flow but enables to simulate thermal refraction due to the horizontal heterogeneity. There are two unknowns in this model: the heat flow and the temperature at the surface.

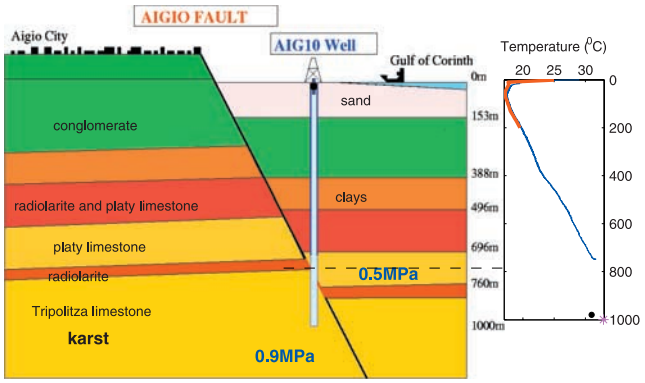

Figure 1. (left) Schematic structural cross-section through Aigio fault and (right) thermal profiles. The two graphs are at the same depth scale. The 1000 m well crosses the Aigio fault at 760 m. The well then penetrates a karst (indicated in yellow) until its bottom. Three thermal profiles have been performed on the well. The IPGP (red thick line) and the GFZ (blue line) thermal logs stop above the fault. The Schlumberger profile (black dot) extends down to 980 m, but was performed only two days after the end of the drilling. OSG log data (mauve asterisk) obtained 7 days later gives a better estimate of the temperature at the bottom of the well.

[18] Figure 3 shows that the upper part of the profile can be well approximated with a heat flow of 53 mW/m^2 and a surface temperature of 15.7°C. However, the model does not fit correctly the measured temperature profile as one gets closer to the fault, as if the temperature gradient is locally increased by 130%.

[19] Is this temperature increase due to a wrong conductivity coefficient? Lumping the heterogeneity of the Pindos nappe layers extending from 496 m to 700 m may not be appropriate and explains the discrepancy at that depth. But the depth interval between 700 m and 760 m is made of homogeneous platy limestone and the discrepancy in temperature gradient between the model and the temperature data is still present. The discrepancy cannot be attributed to an inaccurate thermal conductivity estimation only.

[20] Is this temperature increase due to heat advected by fluid circulation along the fault? Long term pressure monitoring suggests that there is no important fluid circulation in the aquifer above the fault. Downhole pressure has been monitored for more than one-year (Figure 4). The pressure evolves in two stages. First, there is a 3-month transient when the two aquifers previously separated by the fault were connected by the opening of the well. The lower overpressurized karst empties itself into the upper aquifer. In a second stage, the pressure stabilizes to a value close to the initial pressure of the karst. The stationarity of the pressure during this last stage suggests that both aquifers are confined, as the pressure disturbance we artificially induced did not recover. From the brevity of the initial transient, we also conclude that the upper aquifer is small and that internal transport within the aquifer cannot disturb its temperature. The advection of heat by flow in the upper aquifer is then negligible.

[1] Auxiliary material data sets are available at ftp://ftp.agu.org/apend/gl/2006gl028931. Other auxiliary material files are in the HTML.

[21] Is this temperature increase correlated to the fault movement? *Lachenbruch and Sass* [1980] predict the heat production rate induced by fault motion as $Q = v_{rel}\,\tau$, where τ is the tangential stress applied on the fault and v_{rel} the relative velocity. To get a crude estimate of stress, we suppose that the load is controlled by gravity, so that $\tau = \rho g z \sin\theta$, where ρ is the rock density, g the gravity acceleration and $\theta = 60°$ is the angle of the fault to the horizontal. Paleoseismologic investigations suggest a slip rate equal to v = 4 mm/yr [*Pantosti et al.*, 2004]. At a depth of 800 m, this gives a heat production rate equal to 0.8 mW/m^2 only, to be compared with a local heat flux of 53 mW/m^2. The fault effect is therefore negligible.

[22] Can this increase be interpreted by a transient induced by the vertical movement of the hanging wall? *Powell et al.* [1988] showed that a vertical subsidence would decrease the temperature gradient in the upper part of the fault. However, because of the movement of the faults lying north to the Aigio fault, the hanging wall is uplifting and not subsiding, invalidating this hypothesis.

[23] Is this ~1.2 °C temperature increase due to the movement along the normal fault, as it put together rocks of different temperatures? The vertical offset of 150 m is equivalent to a thermal anomaly of 3.3°C. But this offset has been accumulated over at least 50 kyr, which corresponds to a diffusion distance of $\sqrt{D_{th} \times t} > 1$ km, with a thermal diffusivity equal to $D_{th} = 10^{-6}$ m^2/s. Another characteristic timescale is the time of the last major earthquake on the fault: 300 yr. It corresponds to a length scale of 100 m compatible with the observation. But the temperature offset the 1-meter slip would induce would be of only 0.02°C. There is then a problem in trading off amplitude and the size scale of the temperature anomaly with this hypothesis.

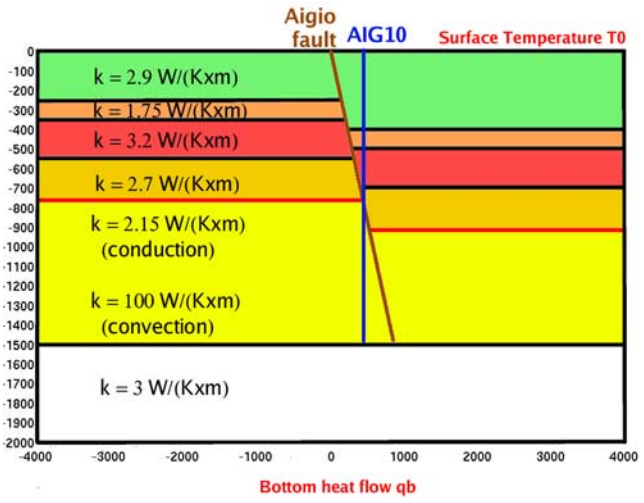

Figure 2. Geometry and parameters of the numerical simulation of the temperature around the fault. The geometry of the model is inspired by Figure 1. The thermal conductivities of the upper layers were measured from cuttings and cores from the borehole (see auxiliary material). The karst in convection is approximated with a high thermal conductivity $k = 100\ W/(K \times m)$ (in yellow). This enables a model of the thermal disturbance near the fault induced by its isothermal boundary, but does not take into account any temperature step through the boundary layer on the convection cell.

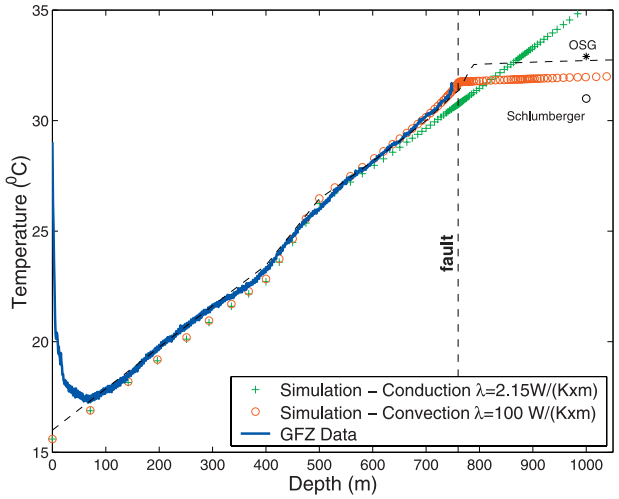

Figure 3. Comparison of thermal data obtained by GFZ (continuous blue line) and the thermal profile produced with the model of Figure 2. The profile obtained for a karst in convection (red circles) fits very well the actual data, in contrast with that computed for a karst in thermal conduction. The model can be refined by modeling the boundary layer at the boundary of the convection cell with an arbitrary 10 m thin layer along the boundary of the karst, with a conductivity of 0.9 W/(K × m). The resulting model (black dashed line) fits better the OSG data (black asterisk) while staying close to the curve computed with the simple convective case.

3. Thermal Refraction Induced by Convection in the Karst Below the Fault

3.1. Evidence for Convection in the Karst

[24] Can we explain the thermal anomaly by fluid circulation below the fault? Both temperature data and theoretical considerations hint that the karst extending below the fault is in a convective state. We will review these arguments in this section.

3.1.1. Indirect Temperature Data

[25] The thermal regime below the fault is only documented by the OSG log. This temperature is much smaller than what predicted by the thermal conduction profile.

[26] That the temperature in the karst is low is supported by the production test of September 2002, when the temperature of the water flowing out of the borehole kept a constant (30 ± 1)°C value for 3 days [*Giurgea et al.*, 2004]. The large flow rate of 50 m^3/h shows that water comes from the overpressurized karst of high permeability. This large flow also suggests that the water has not cooled much while flowing to the surface. This is further confirmed by the fact that the temperature did not change when we diminished the flow rate by 2.

[27] The temperature in the karst seems therefore lower what than predicted for a pure conduction model. However, we miss the measurement of a low temperature gradient to

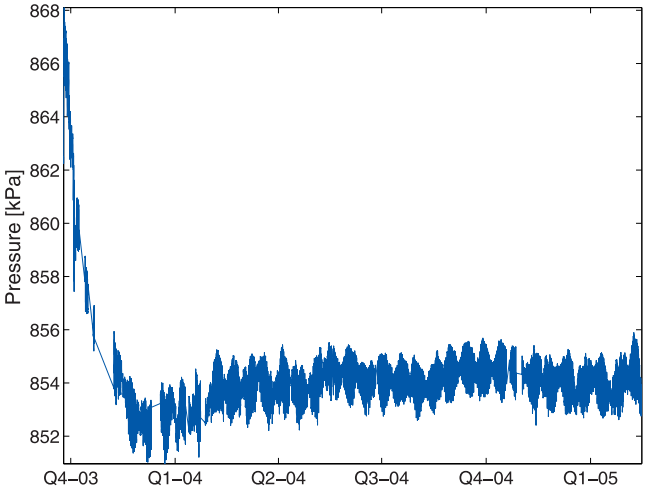

Figure 4. Pressure data at the wellhead of the AIG10 borehole was recorded for more than one year. After a transient induced by the installation of the sensor, the pressure is stationary, indicating that no significant flow crosses the aquifers.

really demonstrate the convection. Hence, we will also use theoretical considerations.

3.1.2. Criteria for the Onset of Convection in a Porous Medium

[28] Convection in a fluid happens when the Rayleigh number (Ra) exceeds a threshold value. For instance, let consider a porous medium placed between two parallel plates separated by a distance H. If the bottom plate is hotter by ΔT, the fluid convects if [*Nield and Bejan*, 1992]:

$$Ra_p = \frac{\alpha \rho g \Delta T K H}{\frac{k}{\rho C_{pf}} \eta} > 4\pi^2 \approx 40 \quad (1)$$

where α is the dilatation coefficient of the fluid, ρ is its density, g the gravity acceleration, K the permeability of the formation, η the dynamic viscosity of the fluid, k the *rock* thermal conductivity and C_{pf} is the *fluid* heat capacity.

[29] The onset of convection requires a minimal value for the aquifer thickness H given by

$$H > \frac{k}{\rho} \sqrt{\frac{4\pi^2 \eta}{\alpha g q_b K C_{pf}}} \quad (2)$$

[30] Tables for water at 30°C [*Lide*, 2005] directly provide the fluid properties: $\eta = 10^{-3}$ Pa × s, $\rho = 10^3$ kg/m^3, $\alpha = 3 \times 10^{-4}$ K^{-1} and $C_{pf} = 4180$ J/(K × kg). We use for the thermal conductivity of the rock the value measured from the cuttings $k = 2.15$ W/(K × m). The heat flux equals $q_b = k\Delta T/H = 53$ mW/m^2.

[31] The permeability K of the karst is so large that a production test in AIG10 borehole was limited by head loss in the borehole. If we take the minimal value of permeability (5×10^{-13} m^2) provided by the production test, the condition of equation (2) is satisfied if the aquifer thickness exceeds 700 m. This critical thickness drops to 400 m with the permeability value $K = 1.5 \times 10^{-12}$ m^2 determined from tidal analysis [*Doan*, 2005]. Both critical heights are smaller than the expected thickness (2000 m) of the Gavovro-Tripolitza zone in which the karst lies. The criterion for convection is likely met.

[32] This is even more likely as we have supposed here that the aquifer boundaries are horizontal. Convection occurs more easily if the boundaries are tilted, as a temperature gradient is applied on the lateral boundaries of the karst [*De Marsily*, 1986].

3.2. Simulation for a Convective Karst

[33] The effect of the convection in the karst below the fault is studied by reusing the numerical simulation detailed in the auxiliary material. Intuitively, because of the convection, the temperature within the karst is uniform. This isothermal volume disturbs the isotherms around the karst. In the configuration of Figure 2, this would induce a local increase in temperature gradient in the hanging wall. The convection in the karst is modeled by assigning a thermal conductivity $k = 100$ W/(K × m). In practice, the exact value of this thermal conductivity is not important: the karst is isothermal and its temperature is controlled by the heat flow at the base of the model and the temperature at the surface. To model the convection in the karst, we do not add any parameters.

[34] Figure 3 compares the simulated profile to the real profile (blue line) for both a karst in convection (red circles) and a karst in conduction (green crosses).

[35] In the case of a karst in convection, the temperature is quasi-uniform within the karst. This disturbs the temperature nearby. This refraction effect is particularly important near the fault, a lateral boundary of the karst. As seen in Figure 3, this effect induces an upward trend that matches better the actual data than the pure conductive case.

[36] Note that we do not consider the temperature offset that occurs at the boundary layer of the convection cell. This induces a sudden temperature change at the crossing of the boundary layer, as given by *Šafanda et al.* [2005]. We can model it by introducing an arbitrary thin zone (here 10 m) of low conductivity (0.9 W/(K × m)). This does not disturb much the initially modeled disturbance, but it enables to fit better the OSG data.

4. Conclusion

[37] The temperature increases anomalously and progressively as one approaches the Aigio fault. The amplitude of this increase is neither explained by thermal refraction, fluid flow on the hanging wall of the fault, transient subsidence, transient heat between moving blocks, nor by the heat generated by this minor fault. The anomaly is better fitted with thermal convection in the footwall karstic limestone. Convection has been rarely described in aquifers outside geothermal areas [*Šafanda et al.*, 2005]. The temperature anomaly near the Aigio fault is an extreme case of coupling between fluid flow and heat flow.

[38] The temperature profile can be explained with a heat flow equal to 53 mW/m^2, but the extrapolation to a regional scale is hampered by the poor knowledge of the flow in the karst. The Aigio Rift is thus not a geothermal area.

[39] **Acknowledgments.** We thank very sincerely Andrea Förster, from GFZ Institute, for agreeing to share with us her temperature data.

We also thank the Laboratoire des Systèmes Dynamiques of IPGP for sharing their expertise on heat flow measurement. We are grateful to Emily Brodsky for fruitful discussions. We thank an anonymous reviewer and August Gudmundsson for their pertinent comments. This study was financed by EU Commission through European project DGLab (contract EVR1-CT-2000-40005).

References

Avallone, A., et al. (2004), Analysis of eleven years of deformation measured by GPS in the Corinth Rift Laboratory area, *C. R. Geosci.*, *336*(4–5), 301–311.

Bernard, P., et al. (1997), The M_s = 6.2, June 15, 1995, Aigion earthquake (Greece): Evidence for low angle normal faulting in the Corinth Rift, *J. Seismol.*, *1*, 131–150.

Cornet, F. H., M. L. Doan, I. Moretti, and G. Borm (2004), Drilling through the active Aigion fault: The AIG10 well observatory, *C. R. Geosci.*, *336*(4–5), 395–406.

De Marsily, G. (1986), *Quantitative Hydrogeology: Groundwater Hydrology for Engineers*, Elsevier, New York.

Doan, M. L. (2005), Étude in-situ des interactions hydromécaniques entre fluides et failles actives: Application au Laboratoire du Rift de Corinthe, Ph.D. thesis, Institut de Physique du Globe de Paris, Paris.

Förster, A., et al. (1997), Application of optical-fiber temperature logging—An example in a sedimentary environment, *Geophysics*, *62*(4), 1107–1113.

Frima, C., et al. (2005), Can diagenetic processes influence the short term hydraulic behaviour evolution of a fault?, *Oil Gas Sci. Technol.*, *60*(2), 213–230.

Giurgea, V., et al. (2004), Preliminary hydrogeological interpretation of the Aigion area from the AIG10 borehole data, *C. R. Geosci.*, *336*(4–5), 467–475.

Koukouvelas, I. (1998), The Egion fault earthquake-related and long-term deformation, Gulf of Corinth, Greece, *J. Geodyn.*, *26*(2–4), 501–513.

Lachenbruch, A. H., and J. H. Sass (1980), Heat flow and energetics of the San Andreas fault zone, *J. Geophys. Res.*, *85*(B11), 6185–6222.

Lide, D. (Ed.) (2005), *CRC Handbook of Chemistry and Physics*, 85th ed., CRC Press, Boca Raton, Fla.

Nield, D., and A. Bejan (1992), *Convection in Porous Media*, Springer, New York.

Pantosti, D., et al. (2004), Paleoseismological investigations of the Aigion fault (Gulf of Corinth, Greece), *C. R. Geosci.*, *336*(4–5), 335–342.

Powell, P., et al. (1988), Continental heat-flow density, in *Handbook of Terrestrial Heat Flow Density Determination*, edited by R. Haenel, R. Rybach, and L. Stegena, pp. 167–222, Springer, New York.

Rettenmaier, D., and I. Unkel (2002), AIG10 - log of the borehole. depth 0–708m (cutting description and rate of penetration - ROP), *Tech. Rep.*, Karlsruhe Univ., Karlsruhe, Germany.

Rettenmaier, D., et al. (2004), The AIG10 drilling project (Aigion, Greece): Interpretation of the litholog in the context of regional geology and tectonics, *C. R. Geosci.*, *336*(4–5), 415–424.

Šafanda, J., et al. (2005), Fluid convection observed from temperature logs in the karst formation of the Yucatán peninsula, Mexico, *J. Geophys. Eng.*, *2*, 326–331, doi:10.1088/1742-2132/2/4/S05.

F. H. Cornet, Department of Seismology, Institut de Physique du Globe de Paris, Casier 89, 4, place Jussieu, F-75005 Paris, France. (cornet@ipgp.jussieu.fr)

M. L. Doan, Earth and Planetary Sciences Department, University of California, Santa Cruz, Earth and Marine Sciences Building, 1156 High Street, Santa Cruz, CA 95064, USA. (mdoan@es.ucsc.edu)